"Effect of non-magnetic Al substitution on the structural and magnetic properties of nanocrystalline Li-Ni-Zn ferrites"

Ashish C. Das[1*], Mithun Kumar Das[1], Mohammad Julhash Miah[1],Sajal Chandra Mazumdar[1], Milon[1], Farid Ahmed[2], A.K.M Akther Hossain[3]

[1]*Department of Physics, Comilla University,Kotbari, Cumilla-3506, Bangladesh*
[2]*Department of Physics, Jahangirnagar University,Savar, Dhaka-1342, Bangladesh*
[3]*Department of Physics, Bangladesh University of Engineering & Technology, Dhaka, Bangladesh*
[*]*Address for correspondence: Ashish C. Das,*

Abstract
Structural and magnetic properties of Al substituted $Li_{0.8}Ni_{0.1}Zn_{0.5}Al_xFe_{2-x}O_4$ ferrites (x=0.0-0.40 in steps of 0.10) prepared by solid state reaction technique have been investigated. Characterization and phase identification of the samples were performed by X-ray diffraction (XRD) technique. The formation of cubic spinel structure without any secondary phase was confirmed by X-ray diffraction analysis. Lattice constant of the compositions decreased with the addition of Al content obeying Vegard's law. The average crystallite size of the samples calculated using Debye-Scherrer equation varied in the range of 19 nm-73 nm. Also, theoretical and bulk density decreased with the substitution of Al content. Besides, porosity showed opposite trend. The real part of initial permeability of the samples decreased the increase in Al content due to replacement of Fe^{3+} ions by Al^{3+} ions which prefer B-(octahedral) to A-(tetrahedral) sites in the AB_2O_4 spinel type ferrites. The higher resonance frequencies were observed with the increase in Al content. The doping of Al^{3+} influences magnetic parameters due to modification of the cation distribution.

Keywords*: Nanocrystalline magnetic materials; X-ray diffraction; Particle size,Magnetic properties*

I. Introduction

From basic and applications point of view, research interest in nano-crystalline spinel ferrites has greatly promoted in last few decades. The studies of nano-sized ferrites have become great important in modern technological applications such as high density magnetic storage, magnetic carries site specific drug delivery, contrast enhancement of MRI, high frequency power application etc. [1-3]. According to their crystal structure, spinel ferrites have naturally two super lattices (i.e. tetrahedral (A) sites and octahedral (B) sites) in AB_2O_4 crystal structure. Preparation conditions, chemical compositions, sintering temperature and quantity of substitution can change the physical properties of spinel ferrites [4]. Various magnetic properties of spinel ferrites depend on chemical composition and cation distribution in tetrahedral A and octahedral B sites because of their AB_2O_4 crystal structure [5]. Lithium ferrites and substituted lithium ferrites are promising materials in the field of microwave devices due to their low cost, high Curie temperature, narrow hysteresis loop and low dielectric loss [6-9]. Many researchers have also investigated that Ni substituted lithium ferrite and Zn substituted lithium ferrite seems to improve magnetic properties [10,11]. In order to find favorable magnetic properties with low losses especially at high frequencies, various authors have studied Zn substituted Li-Ni ferrites and Ni substituted Li-Zn ferrites [12,13].Recently aluminum has been shown to have an influence on the magnetic and dielectric properties of ferrite [14-15]. The Al doped Ni ferrite is promising materials for a wide range of application at radio and microwave frequencies where dielectric and magnetic losses are required to be minimum [16-18]. Several researchers have studied Ni-Zn-Al [19], Li-Co-Ti-Al [20], Mn-Ni-Zn-Al [21]. To the best of our knowledge, no literature is found on Al substituted $Li_{0.4}Ni_{0.1}Zn_{0.5}Al_xFe_{2-x}O_4$. Therefore, in the present study, the effect of Al substitution on the physical and magnetic properties of $Li_{0.8}Ni_{0.1}Zn_{0.5}Al_xFe_{2-x}O_4$, prepared by standard solid state reaction technique has been investigated.

II.Experimental

2.1 Sample preparation

The Al substituted Li-Ni-Zn ferrites with chemical formula $Li_{0.8}Ni_{0.1}Zn_{0.5}Al_xFe_{2-x}O_4$(x=0.00,0.10,0.20,0.30 and 0.40) were prepared by using the standard solid state reaction technique. Powder of Li_2O(99.9%), NiO(99.9%), ZnO(99.9%) and Al_2O_3(99.9%) were used as starting materials and weighted

---

according to the stoichiometric ratio. These stoichiometric amounts of power were mixed and grinded thoroughly by hand. The grinded powers were calcined in air at 600^0C for 5 hours to obtain final product. The calcined powders were then grinded into the fine powders. The fine powders were pressed uniaxially into disk-shaped and toroid-shaped samples. The samples were finally sintered at 1150^0C for 6 hours in air. For sintering process, the heating and cooling rates were 5^0C/min.

2.2 Characterization

The structural characterization of theferrite powders was observed by an X-ray diffractometer() with Cu K_α radiation (λ=0.1540598 nm).The lattice parameter of a cubic sample was calculated by using the formula: $a = \sqrt{h^2 + k^2 + l^2}$ where, a is the lattice parameter, (hkl) are the Miller indices of the crystal planes and d is the inter-planar spacing. The exact lattice constant for each composition was determined by Nelson-Riley function [22]. The crystallite size of the prepared samples were investigated by X-ray diffractometer.

The bulk density, ρ_B, of the samples was calculated using the formula: $\rho_B = \frac{M}{\pi r^2 t}$, where M is the mass of the sample, r is the radius and t is the thickness of the disk-shaped samples.The theoretical density, ρ_{th}, was determined using the expression: $\rho_{th} = \frac{8M_A}{N_A a_0^3}$, Where N_A is the Avogadro's number, M_A is the molecular weight of the samples and a_0 is the lattice constant.The porosity, P, was calculated from the relation: $P(\%) = \frac{\rho_{th} - \rho_B}{\rho_{th}} \times 100$.

The initial permeability spectra as a function of frequency were investigated by a precision impedance analyzer (Wayne Kerr, Model No. 6500B). The complex permeability measurements on toroid-shaped samples were performed at room temperature in the frequency range 100 Hz- 120MHz.The real part (μ_i') and the imaginary part (μ_i'') of the complex permeability was calculated using the following relations: $\mu_i' = \frac{L_s}{L_0}$ and $\mu_i'' = \mu_i' \tan\delta$,where L_s is the self-inductance of the sample core and L_0 is derived by the following relation,[$L_0 = \frac{\mu_0 N^2 S}{\pi \bar{d}}$] [23], where L_0 is the inductance of the winding coil without the sample core, N is the number of turns of the coil (N=4), S is the area of cross section and $\bar{d} = (\frac{d_i + d_0}{2})$ is the mean diameter, where d_i and d_0 are the inner and outer diameter of the toroidal sample respectively. The relative quality factor (RFQ) was calculated from the relation:RFQ $= \frac{\mu_i'}{\tan\delta}$[24], where tan δ is the loss factor.

III.Results and Discussions

3.1 Lattice constant, particle size, density and porosity of the samples

The X-ray diffraction (XRD) patterns of Al^{3+} ion substituted various $Li_{0.8}Ni_{0.1}Zn_{0.5}Al_xFe_{2-x}O_4$ ferrites sintered at 1150^0C are shown in Fig. 1.
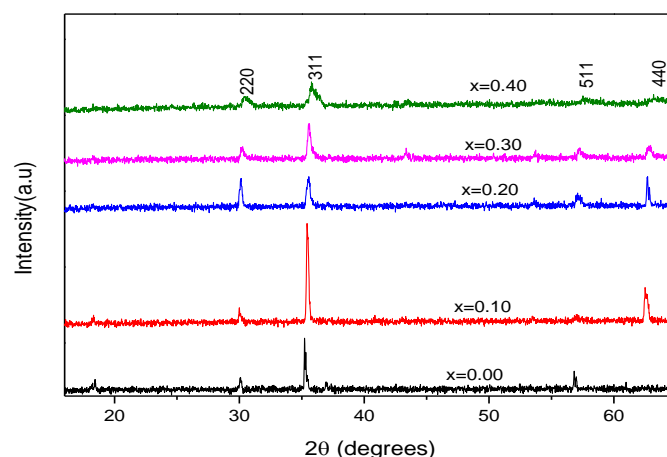

Fig. 1: XRD diffraction pattern for various $Li_{0.8}Ni_{0.1}Zn_{0.5}Al_xFe_{2-x}O_4$ sintered at 1150^0C

The XRD analysis confirms the formation of single phase cubic spinel structure with the absence of any secondary phase. By analyzing the XRD patterns, the positions of the peaks for all compositions match well with the characteristic reflections of spinel structure type ferrites reported earlier [25]. Slightly broader (311) peak in the XRD pattern of the calcined powders confirms that nano-sized particle is formed. The lattice constant, theoretical density, bulk density and porosity for all samples are given in Table 1.

Table 1: The lattice constant, particle size, density, porosity and natural resonance frequency for various $Li_{0.8}Ni_{0.1}Zn_{0.5}Al_xFe_{2-x}O_4$.

Al Content x	Lattice constant a(A^0)	Particle size D(nm)	Theoretical density, ρ_{th}(gm/cm^3)	Bulk density, ρ_B(gm/cm^3)	Porosity P(%)	Resonance frequency f_r(MHz)
0.00	8.43957	73	4.8	4.38	8.7	2.56
0.10	8.39541	68	4.8	4.32	9.93	2.82
0.20	8.37879	44	4.77	4.02	15.84	3.23
0.30	8.36381	42	4.74	3.88	18.04	4.01
0.40	8.28955	19	4.72	1.9	59.68	

The lattice constant (a_0) of various $Li_{0.8}Ni_{0.1}Zn_{0.5}Al_xFe_{2-x}O_4$ compositions were plotted as a function of Al content shown in Fig. 2.
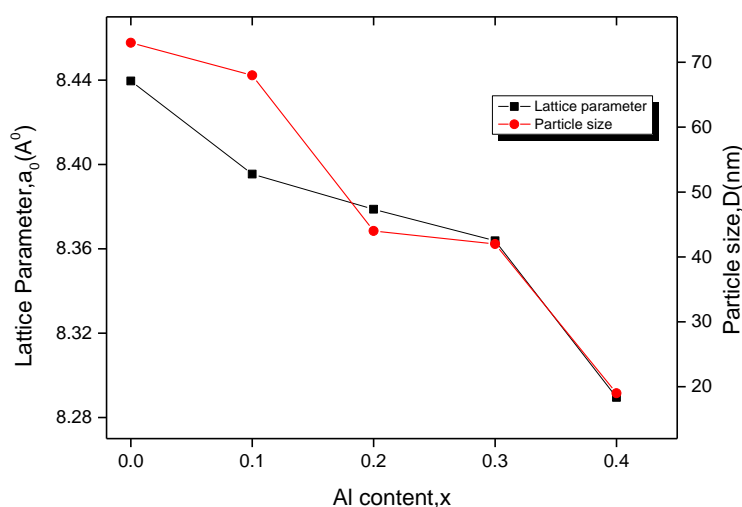

Fig. 2: The variation in lattice constant and particle sizes as a function of Al content.

From this figure, it is found that the lattice constant is slightly decreased with the increase of Al^{3+} content. The decrease in lattice constant with Al^{3+} ion substitution can be explained on the basis of Vegard's law [26]. The law explains the linear variation in lattice constant with the ionic radii of the doped and the replacing ion. In this study Fe^{3+} ion is substituted by Al^{3+} ion. As the ionic radius of Al^{3+} (0.51A˚) ion is smaller than that of Fe^{3+} (0.67 A˚) ion, the substitution of Fe^{3+} ions with Al^{3+} results in a decrease in the lattice constant of the ferrites. Similar results were observed by R.A.Bugadet al (2013) [27] and K. Vijaya Kumar et al (2015) [28].

The average particle sizes are evaluated from the highest intense diffraction peak (311) of the XRD pattern by using the Debye-Scherrer formula[29], $D = {0.9\lambda}/{\beta cos\theta}$, where λ is the wave length of X-ray, θ is the angle of the incident beam in degree and β is the full width at half maximum (FWHM) of the fundamental reflection (311) in radian. The average crystallite sizes of the particles are found to be in the range of 19-73 nm, which are tabulated in Table 1. The particle size of various $Li_{0.8}Ni_{0.1}Zn_{0.5}Al_xFe_{2-x}O_4$ ferrites for a fixed sintering temperature has been decreased with increasing Al^{3+} doping as shown in Fig. 2. Similar observations are reported by KwangPyoChae et all (2012) [20].

Density has been become important in controlling the properties of nano-sized ferrites. The impact of Al^{3+} content on the ρ_B and P for various $Li_{0.8}Ni_{0.1}Zn_{0.5}Al_xFe_{2-x}O_4$ compositions sintered at 1150^{0}C are shown in Fig. 3.
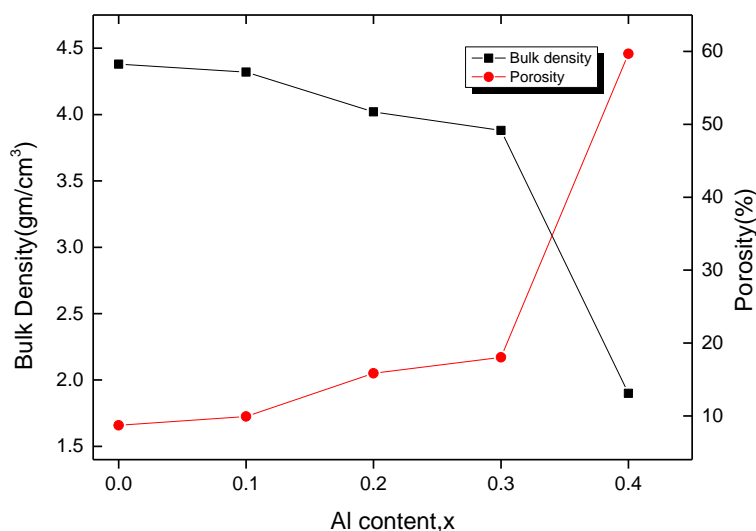
Fig. 3: Bulk density and porosity of various $Li_{0.8}Ni_{0.1}Zn_{0.5}Al_xFe_{2-x}O_4$ sintered at 1150^0C

It is obtained from this figure that ρ_B decreases and porosity increases with increasing Al^{3+} content. This phenomenon can be explained on the basis of the atomic weight of constituent atoms. The atomic weight of Al (26.982 amu) is much less than that of Fe (55.845 amu) [30].The decrease in the values of density may be due to intergranular/intragranular porosity resulting from discontinuous grain growth [31]. Gain growth and densification are closely connected according to the Lange and Kellet [31]. The values of theoretical density (ρ_{th}), bulk density (ρ_B) and porosity (P) for all samples are tabulated in Table 1. ρ_{th}decreases with the enhancement of Al content due to the molecular weight of each composition reduces with the addition of Al^{3+} content. From Table 1, it is observed that the values of theoretical density are higher than the values of bulk density. This may be due to the existence of pores in the samples. Similar trends are reported by Ajmal and Maqsood for Ni-Zn ferrites [33]. The porosity of the samples enhances with the addition of Al^{3+} content. This is due to the lower density of Al^{3+} ions.The increment of porosity can also be explained on the basis of particle size. It is explained that the size of the particles decreases, the porosity increases in the range of 8.7-59.68% [34].

3.2 Initial permeability as a function of frequency
The variation of real part of complex initial permeability ($\mu_i^{'}$) for Al substituted various $Li_{0.8}Ni_{0.1}Zn_{0.5}Al_xFe_{2-x}O_4$ compositions sintered at 1150^0C in the frequency range 100 Hz-120 MHz is shown in Fig. 4.
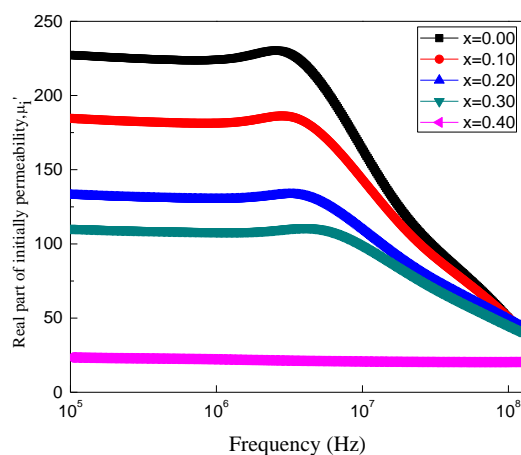

Fig. 4: The frequency dependence real part of initial permeability ($\mu_1^{'}$) for various $Li_{0.8}Ni_{0.1}Zn_{0.5}Al_xFe_{2-x}O_4$ sintered at 1150^0C.

It is observed that μ_i' reduces with the addition of Al^{3+} content. The maximum value of μ_i' is found for parent composition. These can be explained on the basis of cation distribution in Al substituted $Li_{0.8}Ni_{0.1}Zn_{0.5}Al_xFe_{2-x}O_4$ samples. It is known that Li^{1+} (non-magnetic), Ni^{2+} (magnetic moment = $2\mu_B$) and Zn^{2+} (non-magnetic) ions occupy B-sites, although Fe^{3+} exist at both A- and B- sites of the AB_2O_4 spinel ferrites [35]. On the other hand, Al^{3+} (non-magnetic) ions prefer octahedral site to tetrahedral site [14,36]. The assumed cation distribution of various $Li_{0.8}Ni_{0.1}Zn_{0.5}Al_xFe_{2-x}O_4$ may be written as, $(Fe_{0.9}^{3+})_A[Li_{0.8}Ni_{0.1}Zn_{0.5}Al_xFe_{1.1-x}]_BO_4$, where the parentheses and square brackets represent A- and B-sites respectively. In the above cation distribution, Li^{1+}, Zn^{2+} and Al^{3+} do not influence on the net magnetic moment. According to the Neel's molecular field theory [37], the A-B super-exchange interaction is prevailing over intra sub-lattice A-A and B-B interaction and the net magnetization is the vector sum of the magnetic moments of the individual A and B sub-lattice i.e. $M = M_B - M_A$. When Al^{3+} ion replaces Fe^{3+} ion and also prefers octahedral to tetrahedral site, then the magnetic moment of B sub-lattices decreases with increasing Al content. This may weaken A-B super interaction due to non-magnetic Al^{3+} ion does not take part in the exchange interaction. Besides, the magnetic moment of A sub-lattices remains constant with the addition of Al content. As a result, net magnetization decreases with increasing Al content. It is known that the μ_i' of polycrystalline ferrite is related to two different magnetizing mechanisms: spin rotation and domain wall motion [38,39], which can be written as $\mu_i' = 1 + \chi_w + \chi_{spin}$, where χ_w and χ_{spin} are domain wall susceptibility and intrinsic rotational susceptibility. χ_w and χ_{spin} may be written as $\chi_w = \frac{3\lambda M_s^2 D}{4\gamma}$ and $\chi_{spin} = \frac{2\pi M_s^2}{K}$, where M_s K, D and γ are the saturation magnetization, total anisotropy, average grain diameter and domain wall energy respectively. As μ_i' is proportionally related with magnetization, it decreases with increasing Al^{3+} doping. In addition, the spinel structure type ferrites are strongly impacted by its composition, additives and grain sizes of the material. The higher the grain sizes, the greater the magnetization and permeability. The variation in μ_i' as a function of frequency is shown in Fig. 4. It is found that the μ_i' of all compositions remain almost constant at a certain frequency range and then μ_i' decreases with increase in frequency. The general characteristic of the initial permeability spectra is that μ_i' remains almost constant at a certain frequency range, while it reduces rapidly to a very lower value at higher frequency. A critical frequency at which the μ_i' remains fairly constant in the frequency range is known as resonance frequency, f_r. The value of resonance frequency for all compositions varies 2.56-4.01 MHz which is tabulated in Table 1.

Beyond the measured frequency range (> 120 MHz), no resonance frequency, f_r is found for $Li_{0.8}Ni_{0.1}Zn_{0.5}Fe_2O_4$. Soft ferrites can be efficiently used below the resonance frequency. It is possible to explain the variation in permeability with frequency according to the Globus model [40]. According to this model, permeability remains constant with frequency as long as there is no phase lag between the applied field and the domain wall displacement. There are two resonance peaks in ferrites: one at lower frequencies (~1MHz) which is due to the domain wall oscillations [41,42] and the other at higher frequencies (~1GHz) which is due to Larmour precession of electron spins[43].

The variation in magnetic loss factor with frequency for various $Li_{0.8}Ni_{0.1}Zn_{0.5}Al_xFe_{2-x}O_4$ compositions sintered at 1150^0C is shown in Fig. 5. It is observed that from this figure, the magnetic loss tangent increases with increasing Al content. Magnetic loss arises due to non-uniform domain wall motion, various domain defects, and variation of flux density and annihilation of domain wall [44]. Beyond the measured frequency range (> 120 MHz), no loss tangent is observed for $Li_{0.8}Ni_{0.1}Zn_{0.5}Al_{0.2}Fe_{1.8}O_4$. The loss factor becomes high at lower frequencies but reduces rapidly with the increase of frequency and at high frequencies it becomes almost remain constant. It is observed that losses are lower at high frequencies due to domain wall motion is existed and the magnetization is forced to change by rotation [45].
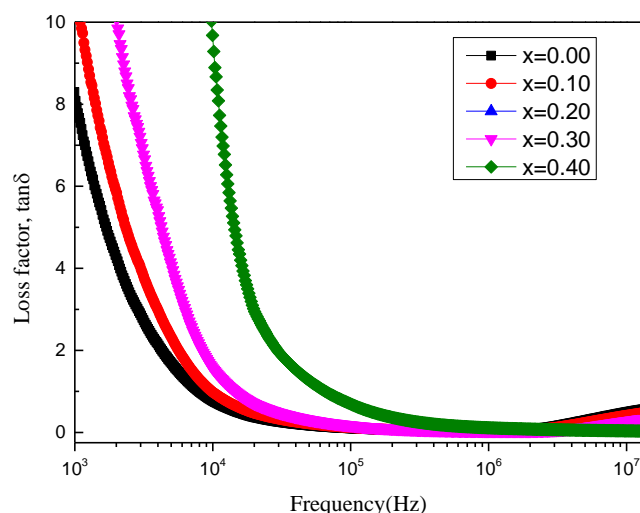
Fig. 5: Loss factor variation with frequency for various $Li_{0.8}Ni_{0.1}Zn_{0.5}Al_xFe_{2-x}O_4$ sintered at 1150^0C

3.3 Relative Quality factor
Fig. 6 illustrates the variation in Q factor as a function of frequency for various $Li_{0.8}Ni_{0.1}Zn_{0.5}Fe_2O_4$ samples sintered at 1150^0C.The Q factor reduces with the addition of Al content.
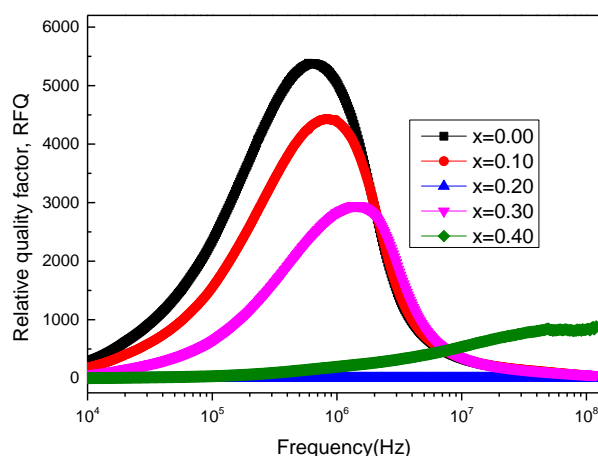
Fig. 6: The variation of quality factor with frequency for various $Li_{0.8}Ni_{0.1}Zn_{0.5}Al_xFe_{2-x}O_4$ sintered at 1150^0C.

This may be due to the growth of imperfection and defects compared to those of other samples.Beyond the measured frequency range (> 120 MHz), no Q factor is observed for $Li_{0.8}Ni_{0.1}Zn_{0.5}Al_{0.2}Fe_{1.8}O_4$ and $Li_{0.8}Ni_{0.1}Zn_{0.5}Al_{0.4}Fe_{1.6}O_4$. For practical application the quality factor is often used as a measure of performance.The Q value increases with an increase in frequency and show a peak at around 1MHz. The highest value of quality factor (Q_{max}= 5294) is observed for parent $Li_{0.8}Ni_{0.1}Zn_{0.5}Fe_2O_4$ composition. This composition also gives lowest magnetic loss.

IV. Conclusions
The substitution of Al on Li-Ni-Zn ferrites influences structural and magnetic properties. The XRD patterns confirm the formation of single phase cubic spinel structure with any absence of secondary phases. The particle sizes are in the range of 19 nm to 73 nm. The lattice constant decreases with the addition of Al content which can be explained on the basis ofionic radii. The bulk density decreases with increasing Al content. On the other hand, porosity shows increasing trend.The initial permeability also shows decreasing trendwith the increase in Al content which can be explained on the basis of cation distribution. The resonance frequency of permeability moves toward higher frequency.This studied material may be helpful for designing high frequency

devices and components. Therefore, Al^{3+} ions play a key role to modify magnetic properties of Li-Ni-Zn ferrites.

References

[1]. M. P. Sharrock, IEEE. Trans. Magn. 25 (1989) 4374.
[2]. D. G. Mitchell, J. Magn. Reson. Imag. 7 (1997) 1.
[3]. S. Dey, A. Roy, D. Das and J. Ghose, J. Magn. Magn. Mater. 270 (2004) 224.
[4]. Yang Bai, Ji Zhou, ZhilunGui, Zhensing Yue, Longtu Li, Mater. Sci. Eng. B.99 (2003) 266.
[5]. R. Peelamedu, C. Grimes, D. Agrawal, R. Roy, J.Mater.Res.18(10)(2003)2292.
[6]. Muthafar F. Al-Hilli, Sean Li, Kassim S.Kassim,JMagn. Magn. Mater. 324 (2012) 873-879.
[7]. A.M. Abo El Ata, M.K. El Nimr, S.M. Attia, D.El. Kony, A.H. Al-Hammadi,J.Magn. Magn. Mater. 297 (2006) 33-43.
[8]. S.A. Jadhav, Mater. Chem. Phys. 65 (2000) 120-123.
[9]. S.T. Assar, H.F. Abosheiasha, M.K. ElNimr,J.Magn. Magn. Mater. 350 (2014) 12-18.
[10]. G. Aravind, M. Raghasudha, D. Ravinder, M. Manivel Raja, S.S. Meena, Pramod Bhat and Mohd. Hashim,Ceramics International (2015) 8842(15)01979-3.
[11]. MosharrafHosainMesbahAhmed, AbulKashem Mohammad AktherHossain, ShamimaChoudhury,Turk J Phys; (2018) 42: 265-272.
[12]. M.A. Islam, Mehedi Hasan and A.K.M. AktherHossain,Journal of Magnetism and Magnetic Materials,(2016) S0304-8853(16)31654-7.
[13]. IbetombiSoibam and Sumitra Phanjoubam, Chandra Prakash, Harish Chandra Verma and R. K. Kotnala; Modern Physics Letters B, Vol. 24, No. 21 (2010) 2277–2282.
[14]. M. Abdullah Dara, Khalid MujasamBatoob, VivekVermac, W.A. Siddiquia, R.K. Kotnalac,∗ Journal of Alloys and Compounds; 493 (2010) 553–560.
[15]. S. P.Waghmarea*, D. M. Borikara, K. G. Rewatkarb; Materials Today: Proceedings 4 (2017) 11866–11872.
[16]. J.Ferre, S.Lemerle, V.Mathet, C.Choppert, Journal of Magnetism and Magnetic Materials260(2003)234–243.
[17]. M.Mozaffari, J.Amighin, Journal of Magnetism and Magnetic Materials 260 (2003) 244–246.
[18]. SumanRashonlel, N.D.Sharma, S.P.Taneja, AjayGupta, Indian Journal of Pure and AppliedPhysics43(2005)44–50.
[19]. H. L. Ge, Z. J. Peng, C. B. Wang‡ and Z. Q. Fu; International Journal of Modern Physics B, Vol. 25, No. 29 (2011) 3881–3892.
[20]. KwangPyoChae, Woo Hyun Kwon, Jae Gwang Lee; Journal of Magnetism and Magnetic Materials; 324(2012)2701–2705.
[21]. A.A. Sattar, H.M. El-Sayed, K.M. El-Shokrofy and M.M. El-Tabey;Journal of Applied Sciences 5 (1): 162-168, 2005.
[22]. J.B. Nelson, D.P. Riley, Proc. Phys. Soc. Lond. 57(1945)160.
[23]. A. Goldman, Handbook of Modern Ferromagnetic Materials, Kluwer Academic Publishers, Boston, U.S.A, 1999.
[24]. B.D. Cullity, C.D. Graham, Introduction to magnetic materials, 2nd edition, Wiley-IEEE Press, 2008.
[25]. A.K.M. AktherHossain,M.Seki,T.Kawai,H.Tabata,J.Appl.Phys.96(2004)1273.
[26]. L.Vegard,Z.Phys.5(17).
[27]. R.A.Bugad, T.R.Mane, C.S. Pawar and B.R.Karche, Golden research thoughts, 2013 vol.2,(11).
[28]. K. Vijaya Kumar1*, D. Paramesh2, P. Venkat Reddy2;World Journal of Nano Science and Engineering, 2015, 5, 68-77.
[29]. H.P. Klug, L.E. Alexander, X-ray Diffraction Procedures for Polycrystalline and Amorphous Materials, John Wiley and Sons, New York, 1997.
[30]. J.F. Shackelford, M.K. Muralidhara, Introduction to Materials Science For Engineers, Sixthed., PearsonEducationInc&, 2005.
[31]. J.E. Burke, Ceramic Fabrication Processes,in:W.D.Kingery(Ed.),Wiley,New York; 1958
[32]. F.F.Lange,B.J.Kellet,J.Am.Ceram.Soc.72(1989)735–741.
[33]. Muhammad Ajmal, AsghariMaqsood,Mater.Sci.Eng.B 139(2)(2007)164–170.
[34]. A.A. Satar, H.M. El-Sayed, K.M. El-Shokrofy, M.M. El-Tabey, J. Appl. Sci. 5 (2005) 162–168.
[35]. B.S. Chauhan, R. Kumar, K.M. Jadhav, M. Singh, J. Magn. Magn. Mater. 283 (2004) 71.
[36]. Sami ullah Rather a, *, O.M. Lemine, Journal of Alloys and Compounds 812 (2020) 152058.
[37]. L. Neel, Ann. Phys. 3 (1948) 137.
[38]. HuJun,YanMi,J.ZhejiangUniv.Sc.6B(6)(2005)580.
[39]. T. Tsutaoka, M. Ueshima, T. Tokunaga, T. Nakamura, K. Hatakeyama, J. Appl. Phys. 78(6)(1995)3983.
[40]. A.Globus,J.Phys.Colloq.38(1977)C1–C17.
[41]. S.H.Kang,H.I.Yoo,J.Appl.Phys.88(2000)4754.
[42]. O.F.Caltun,L.Spinu,IEEETrans.Magn.37(4)(2001)2353.
[43]. G.T.Rado,R.W.Wright,W.H.Emerson,A.Terris,Phys.Rev.88(1952)909.
[44]. Md. Mamun-Or-Rashid1, Humayun Kabir2*, Mashudur Rahaman3, Md. Abdul Gafur4, A.T.M.K. Jamil1, Syed Jamal Ahmed1, Abdulla Al Noman1, Farid Ahmed2, IOSR Journal of Applied Physics (IOSR-JAP), e-ISSN: 2278-4861.Volume 7, Issue 5 Ver. I (Sep. - Oct. 2015), PP 76-83.
[45]. D. Jiles, Introduction to Magnetism and Magnetic Materials (London Chapman 1998).